RSC Advances

ROYAL SOCIETY OF CHEMISTRY

www.rsc.org/advances

A table of contents entry

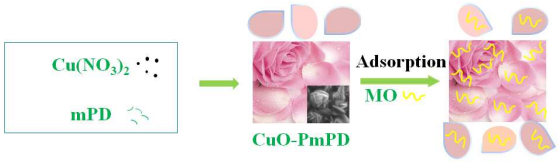

One-step synthesised CuO-PmPD flowerlike composites exhibite a superior adsorption capacity for MO.

Uniform copper oxide-poly(*m*-phenylenediamine) microflowers: synthesis and application for the adsorption of methyl orange

Tingting Guo, Xinyuan Kang, Tingting Zhang, Fang Liao*

A rapid, templateless, surfactantless approach is proposed to prepare copper oxide-poly(*m*-phenylenediamine) (CuO-PmPD) microflower composites by simply mixing of aqueous Cu $(NO_3)_2$ and *m*-phenylenediamine (mPD) at 10 °C. The concentrations of reactants are found to play an important role on the formation of CuO-PmPD morphologies. The morphologies of the composites can be varied from microflowers to spheres by changing the concentrations of reactants. Moreover, the CuO-PmPD microflower composites exhibit a superior capacity for methyl orange (MO) adsorption.

Keywords: CuO-PmPD composites; microflower; methyl orange.

1. Introduction

During the past years, a great deal of research interest has been focused on one-dimensional (1D) structures (rods, wires, tubes and belts), owing to their unique properties and potential to revolutionize broad areas of nanotechnology and microtechnology.[1-3] However, the assembly and integration of 1D materials into three-dimensional (3D) arrays or hierarchical structures are desirable for many applications, such as drug delivery, sensing, energy conversion and storage, light-emitting displays, catalysis and adsorption.[4-8] Various physical and chemical routes have been developed to fabricate 3D hierarchical ordered structures[9-11] for facile addressing, transport, contact and detection. However, these methods usually require rigorous conditions: either high temperatures or special techniques, which possibly lead to high cost and further limit their potential applications. Therefore, the fabrication of desired hierarchical micro/nanostructures via rational, simple and cost-effective technique remains a significant challenge.

Polymers based on aniline derivatives have also been extensively investigated[12], among which poly(phenylenediamine) (PPD) is one of the most studied conducting polymers due to their high thermostability and sensitivity.[13, 14] As a result, intensive efforts have been put into synthesizing PPD with various morphologies including microparticles, nanobelts, and microfibrils, *et al.*[15-18] to meet the demand for design and construction of devices.[19] Min and co-workers reported shape-controlled method for synthesis of poly(*p*-phenylenediamine) (PpPD) microstructures using a UV lamp as the oxidation energy source and poly(*N*-vinylpyrrolidone) (PVP) as the surfactant.[20] Zhang *et al*. fabricated poly(*m*-phenylenediamine) (PmPD) core-shell nanoparticles by directly mixing of aqueous silver nitrate and *m*-phenylenediamine (mPD) solutions at room temperature.[21] So far, a variety of PPD based micro/nanostructures also have been successfully synthesized through template method,[22] electropolymerization method,[23] photopolymerization method [24] and so on. However, the simple, economical and productive synthesis approach is few. Despite Wang et al. prepared poly(*o*-phenylenediamine) (PoPD) microfibrils using cupric sulfate as a facile oxidant in the absence of any external surfactant,[25] the PPD hierarchical structures that are advantageous for adsorption have not been produced by the simple and economical method. Moreover, to the best of our knowledge, the synthesis of copper oxide-poly(*m*-phenylenediamine) (CuO-PmPD) flowerlike composites via a liquid synthesis process has not yet been reported.

Herein, we demonstrate the preparation of uniform CuO-PmPD flowerlike composites by directly mixing of Cu $(NO_3)_2$ and mPD aqueous solution at 10 °C. This simple and cost-effective process does not need any catalysts and surfactants. Meanwhile, the morphology of CuO-PmPD composites can be modulated under the control of reactant concentrations. In our research, a series of techniques were applied to characterize the crystallographic

phase, morphology, microstructure and adsorption of the products. More importantly, the as-synthesized CuO-PmPD flowerlike composites exhibit a great promise to remove methyl orange (MO) from aqueous solution.

2. Experimental

2.1 Materials and apparatus

Cu $(NO_3)_2$ and MO were purchased from Shanghai Chemical Factory (Shanghai, China). HNO_3, NaOH, $(NH_4)_2S_2O_8$ and mPD were purchased from Kelong (Chengdu, China). All the chemicals were analytic reagent grade and used without further purification. The water used throughout all experiments was purified through a Millipore system.

The crystallographic phase, microstructure, thermal stability, morphology and element analyse of sample 1 were characterized by Fourier transform infrared spectroscopy (FTIR, Thermo Scientific Nicolet 6700 FT-IR Spectrometer), thermogravimetric analysis (TGA, STA 449 F3 Jupiter), X-ray photoelectron spectroscopy (XPS, XSAM 800 spectrometer), and scanning electron microscope (SEM, JEOL JSM-6510LV) coupled with an energy-dispersive X-ray spectroscopy (EDS, Oxford instruments X-Max). Brunauer-Emmett-Teller (BET) surface area of the samples were measured by a micromeritics Analyser (ASAP, Autosorb-IQ-MP).

The concentration of leached Cu^{2+} in the supernatant was determined by a WFX-120 atomic absorption spectroscopy (AAS, Rayleigh Analytical Instrument Corp.).

2.2 Preparation of CuO-PmPD composites

The CuO-PmPD flowerlike composites were prepared as follows: 2 mL of mPD aqueous solution was directly introduced into 8 mL of Cu $(NO_3)_2$ aqueous solution at 10 °C. The concentrations for mPD and Cu $(NO_3)_2$ were equal at 0.1 M, 0.2 M, 0.4 M for sample 1, 2, 3 (the molar ratio of mPD to Cu $(NO_3)_2$ is 1:4). The color of the mixture gradually changed from blue to dark. Ten hours later, a large quantity of dark precipitates were observed. The formed precipitates were washed with distilled water for three times, and then dried at 50 °C in vacuum for further characterization.

2.3 Adsorption experiments

The adsorption of MO on CuO-PmPD composites (sample 1) have been examined by a series of experiments. A known weight of CuO-PmPD (5mg) was equilibrated with 20 mL of 65 mg/L aqueous MO solution in a 100 mL Erlenmeyer flask at 30 °C using a shaking bath. The initial pH was adjusted with 0.1 M HNO_3 or 0.1 M NaOH. After shaking for 1 h to ensure full equilibration, the suspension was separated by centrifugation and the obtained supernatant was estimated by UV-Vis absorption spectroscopy (UV, Tsushima Japan 2550 UV-Vis spectrometer) at the maximum absorbance (464 nm).

The adsorption capacity was calculated from the following expressions:

$$Q_e = \frac{(C_o - C_e)V}{m} \quad (1)$$

Where Q_e is adsorption capacity of the adsorbent at equilibrium (mg/g), C_o and C_e are the initial and equilibrium concentrations of MO (mg/L) respectively, V is the volume of solution (mL) and m is the dose of CuO-PmPD composites(g).

3. Results and discussion

3.1 Characterization of CuO-PmPD composites

Figure 1 shows typical SEM images of the products (sample 1). The low-magnification SEM image (Figure 1A) clearly indicates a large amount of microflowers composed by microplates are formed in this process. A close

view of this sample shown in Figure 1B further reveals that these microplates have diameters ranging from 3 to 4 μm, and thickness about 350 nm.

EDS analysis (Figure 2) shows the chemical composition of the products (sample 1). The peaks corresponding to C, N, O, and Cu elements are observed, indicating the possible existence of CuO and PmPD in thus formed products.

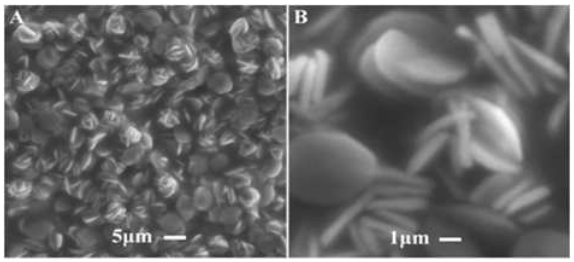

Figure 1 (A) Low and (B) high magnification SEM images of the products synthesized with 0.1 M mPD and 0.1M Cu $(NO_3)_2$ aqueous solution (the molar ratio of mPD to Cu $(NO_3)_2$ is 1:4)

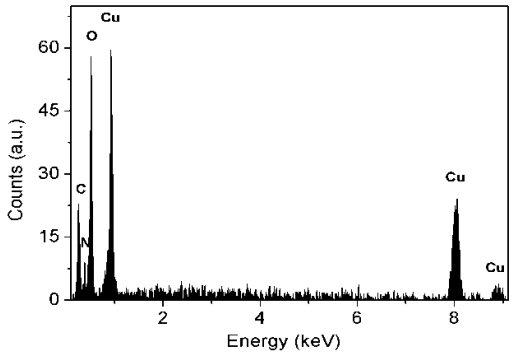

Figure 2 EDS image of the products synthesized with 0.1 M mPD and 0.1M Cu $(NO_3)_2$ aqueous solution (the molar ratio of mPD to Cu $(NO_3)_2$ is 1:4)

The FTIR spectrum of the products (sample 1) is shown in Figure 3. The adsorption peaks around 3400 cm^{-1} correspond to the N-H stretching mode.[13] The peaks at 1624 and 1427 cm^{-1} are assigned to C-N and C-C stretching vibrations in phenazine structure, respectively.[26] The peak at 1343 cm^{-1} is associated with the C-N stretching in the benzenoid and quinoid imine units.[27] The adsorption peak at 1041 cm^{-1} is ascribed to the aromatic C-H in plane bending mode.[28, 29] The results agree well with the FTIR spectra of PPD previously reported.[30-32] The following consideration is Cu-O vibrations, the adsorption peaks in Figure 3 are consistent with vibration frequences of Cu-O in the range of 500 cm^{-1} and above,[33] proving the CuO may be produced.

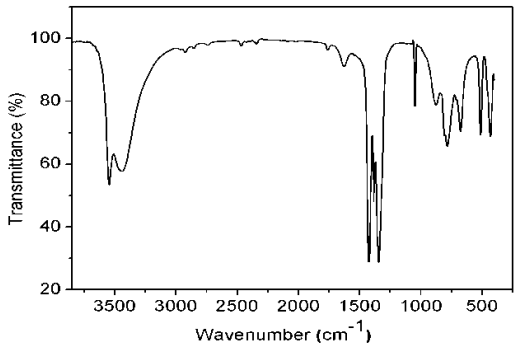

Figure 3 FT-IR spectrum of the products synthesized with 0.1 M mPD and 0.1M Cu $(NO_3)_2$ aqueous solution (the molar ratio of mPD to Cu $(NO_3)_2$ is 1:4).

Figure 4 exhibits Cu_{2p} XPS spectra of the products (sample 1). The Cu_{2p} spectra show two main peaks located at about 933.3 and 953.3 eV, corresponding to $Cu_{2p3/2}$ and $Cu_{2p1/2}$, respectively, which is in agreement with the standard spectrum of CuO.[34] And the peak at 941.6 eV is attributed to a satellite peak. All the above results further indicate the successful fabrication of CuO-PmPD flowerlike composites.

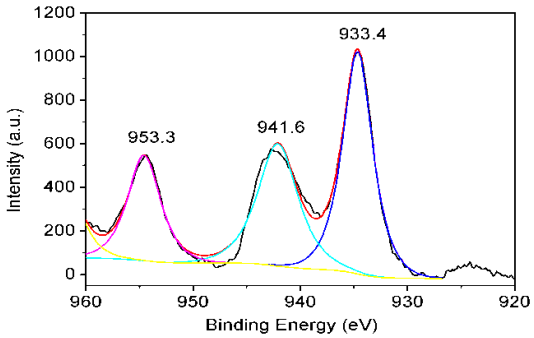

Figure 4 Cu_{2p} XPS spectra of the products synthesized with 0.1 M mPD and 0.1M Cu $(NO_3)_2$ aqueous solution (the molar ratio of mPD to Cu $(NO_3)_2$ is 1:4).

Thermogravimetric analysis (Figure 5) of the CuO-PmPD composites (sample 1) was carried out under nitrogen atmosphere with heating rate of 10 °C per minute. The CuO-PmPD composites underwent a three-stage degradation: (a) loss of water (about 100 °C); (b) decomposition of NO_3^{-1} (about 275 °C); (c) degradation of polyaniline backbone, benzene and quinonoid ring opening (after 400 °C). [35, 36] It can been seen that 47% of weight is still remained as the temperature increases to 800 °C, so the thermal stability of CuO-PmPD flowerlike composites is really good.

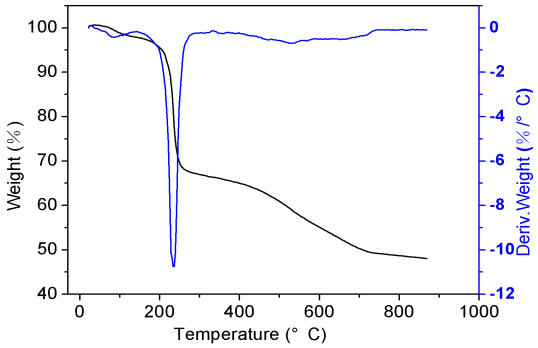

Figure 5 TG and DTG curves of the products synthesized with 0.1 M mPD and 0.1M Cu $(NO_3)_2$ aqueous solution (the molar ratio of mPD to Cu $(NO_3)_2$ is 1:4)

To evaluate the surface areas and porous properties of the samples, nitrogen adorption and desorption measurements were performed. The BET surface area of sample 1 is 23.207 m^2/g, which is bigger than that of sample 2 (5.583 m^2/g) or sample 3 (3.773 m^2/g). The larger BET surface area of sample 1 is attributed to its microflower morphology, and it is advantageous for the adsorption process.

3.2 Shape control of the CuO-PmPD composites

Remarkable changes in self-assembly behavior of the hierarchical microstructures were investigated with different concentrations of reactants (Figure 6). Figure 6A shows typical SEM image of the composites (sample 1) that were synthesized using 0.1 M mPD and 0.1 M Cu $(NO_3)_2$ aqueous solution. It can be clearly seen that the products contain microflowers composed by well-defined microplates. Interestingly, when the concentrations of mPD and Cu $(NO_3)_2$ aqueous solution equally increase to 0.2 M (sample 2), the microplates are interconnected together to form symmetrical hydrangea-shaped microspheres (Figure 6B). As the reactant concentrations are further increased to 0.4 M (sample 3), the microspheres are also formed. But the surfaces of them are much smoother than those of sample 2 (Figure 6C). It should be pointed out that the reactant concentrations have little effect on the size of the products (1.5-3 μm). The microplates are likely to attach each other and welding in terms of energy reduction, which could occure whenever the adjacent CuO-PmPD microplates are overlapped or in physical contact with each other. And the higher reactant concentrations can make the attachment much easier. Therefore, it is reasonable to conclude that microplate attachment and welding may contribute to the morphology evolution of CuO-PmPD from microflowers to microspheres.

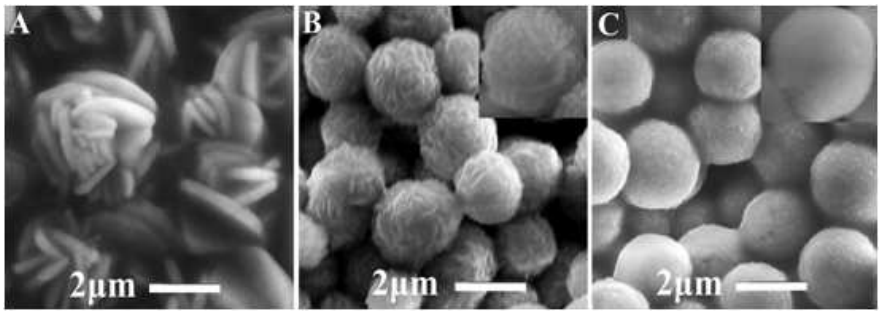

Figure 6 SEM images of CuO-PmPD composites at different concentrantions (A) 0.1 M, (B) 0.2 M, and (C) 0.4 M (the molar ratio of mPD to Cu $(NO_3)_2$ to is 1:4)

3.3 Adsorption of MO

To demonstrate the adsorption application of CuO-PmPD composites, a series of experiments based on the adsorption of MO have been examined. It is excited to find that the prepared CuO-PmPD composites exhibit a superior adsorption capacity for MO. Besides π-π stacking interactions between MO molecules and CuO-PmPD composites, electrostatic adsorption is another important factor for the adsorption capacity of CuO-PmPD composites towards MO.

Effect of pH. The acidity of solution can affect the adsorption capacity of CuO-PmPD composites for MO, that is because both the charges of CuO-PmPD's backbone and MO can be strongly affected by pH value of solution. The chemical structures of MO at different pH values are shown in Figure 7. The acidity-dependent mass uptakes for MO on the CuO-PmPD samples are illustrated in Figure 8. It can be seen that the adsorption capacity of CuO-PmPD samples toward MO increases with increasing pH and reaches a maximum at the pH value of 6.5. It can be attributed to the strong electrostatic adsorption between the negatively charged MO and positively charged CuO-PmPD composites in the aqueous solution. However, the adsorption capacity decreases when the pH is further increased. This is most likely due to the fact that the CuO-PmPD composites can be dedoped easily in alkali solution and consequently changed into neutral materials. The electrically neutral materials then have no electrostatic interaction with ionic MO molecules. Therefore, the solution at pH 6.5 is selected as the medium for the adsorption process.

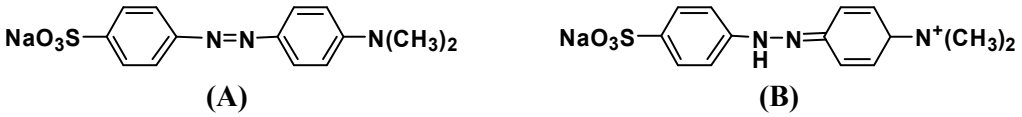

(A) (B)

Figure 7 The structures of MO molecule at different pH values (A) pH > 4.4 and (B) pH < 3.1.

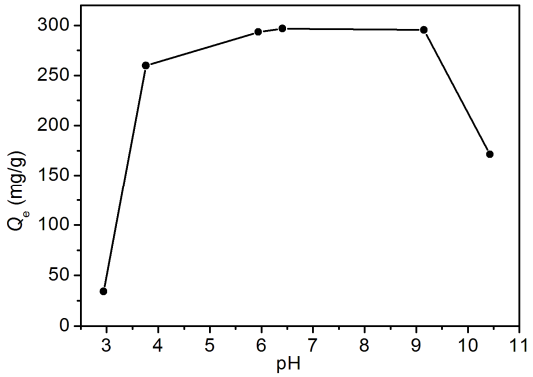

Figure 8 Effect of initial pH values (2.9, 3.8, 6.0, 6.5, 9.1, and 10.4) on the adsorption capacity of MO on CuO-PmPD composites. [MO]=65 mg/L; *t* =1.0 h; *T*=30 °C; the dose of each CuO-PmPD is 5mg.

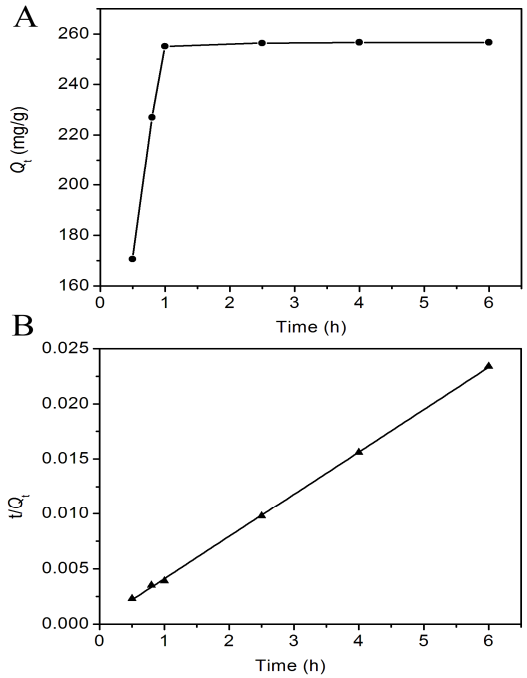

Figure 9 (A) Adsorption kinetics curve and (B) pseudo-second-order kinetic plot for the adsorption of MO on CuO-PmPD composites. [MO] = 65 mg/L; pH=6.5; *T*=30 °C; the dose of each CuO-PmPD is 5mg.

Kinetic. The adsorption kinetic of MO on CuO-PmPD composites was investigated by real-time monitoring as shown in Figure 9. It is clearly observed that the adsorption capacity of CuO-PmPD composites become fully saturated in an hour, and then does not increase any more (Figure 9a). Figure 9b shows the kinetic plot for the adsorption of MO by CuO-PmPD composites according to the pseudo-second-order equation:

$$\frac{t}{Q_t} = \frac{1}{K_2 Q_e^{\ 2}} + \frac{t}{Q_e} \qquad (2)$$

Where Q_e and Q_t are the mass uptake of MO adsorbed on CuO-PmPD composites at equilibrium and different time intervals, respectively, and K_2 is the rate constant (g · min · mg^{-1}). Good linear correlation is observed in Figure 9b (R^2 = 0.9993), suggesting that the reaction follow pseudo-second-order kinetics. In addition, the value of Q_e can be calculated from the slope, *i.e.* 264.55 mg/g for the flowerlike CuO-PmPD composites, which agree well with the experimental value.

Isotherm. Figure 10 shows the adsorption isotherm and typical Freundlich-type isotherm of MO on CuO-PmPD composites at different concentrations of MO ranging from 10 to 80 mg/L. Note that adsorption amount of MO increases quickly with the increased initial concentration of MO and flattens later (Figure 10a), which agrees well with the nature of Freundlich equation. It is further proved by fitting the experimental equilibrium adsorption data using the Freundlich equation:

$$Q_e = K_f C_e^{1/n} \qquad (3)$$

$$\log(Q_e) = \log K_f + \frac{1}{n}\log C_e \qquad (4)$$

Where C_e and Q_e are equilibrium concentration (mg/L) of MO and equilibrium adsorption capacity (mg/g) of CuO-PmPD for MO, respectively. K_f and n are Freundlich constants. The result shows that the adsorption of MO molecules on CuO-PmPD composites well follows the Freundlich isotherm (R^2 = 0.9915), as shown in Figure 10b. The Freundlich constants for adsorbents are also calculated and presented in Table 1.

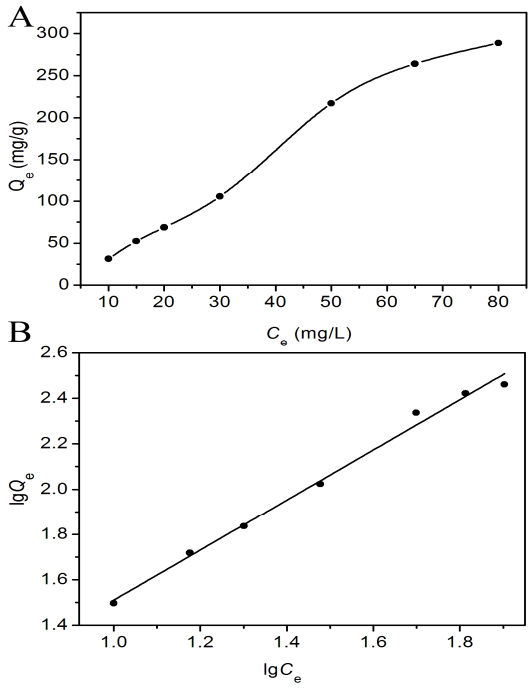

Figure 10 (A) Adsorption isotherms of MO on CuO-PmPD and (B) Plot of lg(Q_e) vs. lg(C_e) for methyl orange adsorption onto CuO-PmPD. pH=6.5; T=30 °C; t=1.0h; the dose of each CuO-PmPD is 5mg.

Sample	K_f	n	R^2
CuO-PmPD	12.7912	0.9010	0.9915

Table 1 Freundlich parameters of CuO-PmPD composites.

Thermodynamics. In order to clarify the thermodynamic performance of MO on CuO-PmPD, we developed an environment-controlled system, in which the temperature is adjusted in the range from 30 to 70 °C (Figure 11). Note that the adsorption capacity of the flowerlike CuO-PmPD decreases as the temperature increases (Figure 11a), indicating the adsorption is an exothermic process. To certify this conclusion, the curve of lg (Q/C_e) versus 1/T for CuO-PmPD composites is obtained (Figure 11b) by fitting the experiments data (R^2=0.9910). The thermodynamic parameters, such as, the change of enthalpy (ΔH^θ), entropy (ΔS^θ) and Gibb's free energy (ΔG^θ), are obtained using the following equations:

$$\log\left(\frac{Q}{C_e}\right) = -\frac{\Delta H^\theta}{2.303RT} + \frac{\Delta S^\theta}{2.303R} \quad (5)$$

$$\Delta G^\theta = -\Delta H^\theta - T\Delta S^\theta \quad (6)$$

As listed in Table 2, the negative value of ΔH^θ obtained from the equation 5 indicates that the adsorption is an exothermic process. Thus the lower temperature makes the adsorption process easier. The negative value of ΔS^θ indicates that there is a decrease in degree of order at the solid/solution interface during the adsorption process. In addition, the negative value of ΔG^θ obtained from the equation 6 confirms spontaneous nature of the adsorption.

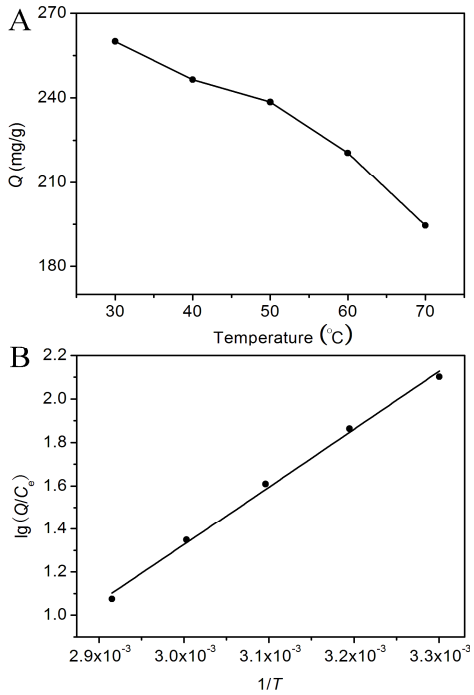

Figure 11 (A) Effect of temperature on adsorption capacity and (B) Plot of lg(Q/C_e) vs. 1/T for MO on CuO-PmPD. [MO] = 65 mg/L; pH=6.5; t=1.0h; the dose of each PmPD-CuO is 5mg.

Temperature (°C)	Δ G^0 (kJ/mol)	Δ H^0 (kJ/mol)	Δ S^0 (J/mol)
30	-26.1	-41.4	-50.5
40	-27.1	-41.4	-45.7
50	-28.0	-41.4	-41.5
60	-29.0	-41.4	-37.2
70	-30.0	-41.4	-33.2

Table 2 Thermodynamic parameters for MO adsorbance on the CuO-PmPD composites

Reusability of adsorbents. To investigate the reusability of the CuO-PmPD adsorbents, the CuO-PmPD composites saturated with MO were first separated by centrifugation, and then regenerated by treatment with 0.5M NaOH at 80 °C according to the reference[37] with a slight modification. Finally, the NaOH-treated CuO-PmPD composites were washed repeatedly with distilled water to neutral, dried, and recycled as described in the adsorption experiment. Figure 12 shows the MO adsorption amount of the CuO-PmPD undergoing four cycles. It can be seen that the adsorption amount of MO on CuO-PmPD composites almost keeps unchanged in the whole cycles, suggesting the as-prepared CuO-PmPD composites can be recycled and reused without loss of their active sites.

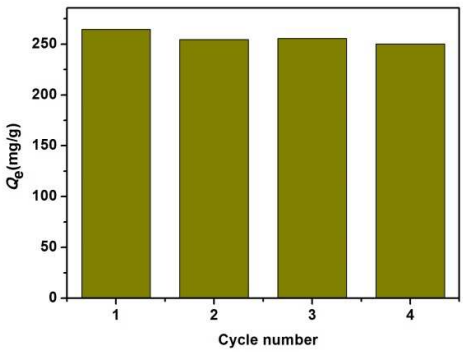

Figure 12 Cyclability of the as-prepared CuO-PmPD adsorbents.

comparison of maximum adsorption capacities. To evaluate the superiority of CuO-PmPD for adsorption, we performed a comparison experiment about maximum adsorption capacities of MO between CuO-PmPD and PmPD adsorbents. The result suggested that CuO-PmPD adsorbents show a stronger adsorption for MO compared with PmPD adsorbents (Figure 1S, ESI†).

3.4 Stability of adsorbents

Considering stability of CuO-PmPD adsorbents at different pH levels, we performed a leaching test in the aqueous solution. 5mg CuO-PmPD was dispersed in 20 mL aqueous solution with pH ranging from 1.0 to 11.0 and agitated in a temperature-controlled shaker at 30 °C for 300 min. Figure 13 shows the concentrations of leached Cu^{2+} under different pH levels. The concentration of Cu^{2+} is negligible at pH over 3.0 and increases significantly when pH is lower than 3.0. At pH 1.0, the concentration of the leached Cu^{2+} is 17.48mg/L. These results imply that CuO-PmPD composites could maintain a good stability in the weak acidic, neutral and alkaline aqueous medium.

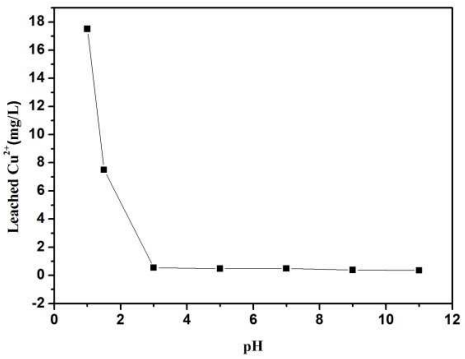

Figure 13 Leached Cu^{2+} content from CuO-PmPD adsorbents under different pH levels.

Conclusions

In summary, we have reported the one-step synthesis of CuO-PmPD flowerlike composites by a direct redox between Cu $(NO_3)_2$ and mPD in an aqueous medium at 10 °C. And the morphology of CuO-PmPD samples can be modulated by changing the concentrations of reactants. As a proof of concept, we demonstrate the successful use of such CuO-PmPD composites as adsorbent for MO. The operational parameters, such as, pH of the solution, equilibrium time, initial concentration of MO, as well as adsorption temperature have been studied during the experiments. The adsorption kinetics and isotherms are well described by pseudo-second-order kinetics and Freundlich model, respectively. The calculated thermodynamic parameters indicate that the adsorption process is feasible, spontaneous and endothermic in nature. Most importantly, the prepared flowerlike composites are insoluble and exhibited a superior adsorption capacity (264.55 mg/g) for MO, suggesting a potential application for the removal of MO from wastewater.

Notes and references

College of Chemistry and Chemical Engineering, China West Normal University. Nanchong 637002, China

*liaozhang2003@163.com

1 Y. Xia, P. Yang, Y. Sun, Y. Wu, B. Mayers, B. Gates, Y. Yin, F. Kim and H. Yan, *Advanced materials*, 2003, **15**, 353-389.
2 C. Rao, G. Gundiah, F. L. Deepak, A. Govindaraj and A. Cheetham, *Journal of Materials Chemistry*, 2004, **14**, 440-450.
3 Y. Li, F. Qian, J. Xiang and C. M. Lieber, *Materials Today*, 2006, **9**, 18-27.
4 H. J. Koo, Y. J. Kim, Y. H. Lee, W. I. Lee, K. Kim and N. G. Park, *Advanced Materials*, 2008, **20**, 195-199.
5 K. C. Popat, M. Eltgroth, T. J. Latempa, C. A. Grimes and T. A. Desai, *Biomaterials*, 2007, **28**, 4880-4888.
6 G. K. Mor, K. Shankar, M. Paulose, O. K. Varghese and C. A. Grimes, *Nano letters*, 2005, **5**, 191-195.
7 X. Feng, J. Zhai and L. Jiang, *Angew Chem Int Ed Engl*, 2005, **44**, 5115-5118.
8 S.-H. Jung, E. Oh, K.-H. Lee, Y. Yang, C. G. Park, W. Park and S.-H. Jeong, *Crystal growth and design*, 2007, **8**, 265-269.
9 S. Sattayasamitsathit, A. M. O'Mahony, X. Xiao, S. M. Brozik, C. M. Washburn, D. R. Wheeler, W. Gao, S. Minteer, J. Cha and D. B. Burckel, *Journal of Materials Chemistry*, 2012, **22**, 11950-11956.
10 L.-P. Zhu, H.-M. Xiao, W.-D. Zhang, G. Yang and S.-Y. Fu, *Crystal Growth and Design*, 2008, **8**, 957-963.
11 L. Vayssieres and M. Graetzel, *Angewandte Chemie*, 2004, **116**, 3752-3756.
12 T. Sulimenko, J. Stejskal, I. Křivka and J. Prokeš, *European polymer journal*, 2001, **37**, 219-226.
13 R. Gangopadhyay and A. De, *Chemistry of Materials*, 2000, **12**, 608-622.
14 E. K. Miller, C. J. Brabec, H. Neugebauer, A. J. Heeger and N. Serdar Sariciftci, *Chemical physics letters*, 2001, **335**, 23-26.
15 X.-G. Li, X.-L. Ma, J. Sun and H. a. Mei-Rong, *Langmuir : the ACS journal of surfaces and colloids*, 2009, **25**, 1675-1684.
16 J. J. Wang, J. Jiang, B. Hu and S. H. Yu, *Advanced Functional Materials*, 2008, **18**, 1105-1111.
17 L. Zhang, L. Chai, H. Wang and Z. Yang, *Materials Letters*, 2010, **64**, 1193-1196.
18 Y. Zhang, L. Wang, J. Tian, H. Li, Y. Luo and X. Sun, *Langmuir : the ACS journal of surfaces and colloids*, 2011, **27**, 2170-2175.
19 Q. Deng and S. Dong, *Journal of Electroanalytical Chemistry*, 1994, **377**, 191-195.
20 Y.-L. Min, T. Wang, Y.-G. Zhang and Y.-C. Chen, *Journal of Materials Chemistry*, 2011, **21**, 6683-6689.
21 Y.-W. Zhang, H.-L. Li and X.-P. Sun, *Chinese Journal of Analytical Chemistry*, 2011, **39**, 998-1002.

22 Y. Yang, Y. Chu, F. Yang and Y. Zhang, *Materials Chemistry and Physics*, 2005, **92**, 164-171.
23 Y. Du, H. Wang, A. Zhang and J. Lu, *Chinese Science Bulletin*, 2007, **52**, 2174-2178.
24 O. Abdulrahman, *Catalysis Science & Technology*, 2012, **2**, 711-714.
25 L. Wang, S. Guo and S. Dong, *Materials Letters*, 2008, **62**, 3240-3242.
26 Q. Hao, B. Sun, X. Yang, L. Lu and X. Wang, *Materials Letters*, 2009, **63**, 334-336.
27 A. Kitani, T. Akashi, K. Sugimoto and S. Ito, *Synthetic metals*, 2001, **121**, 1301-1302.
28 K. Mallick, M. J. Witcomb, A. Dinsmore and M. S. Scurrell, *Langmuir : the ACS journal of surfaces and colloids*, 2005, **21**, 7964-7967.
29 A. Drelinkiewicz, M. Hasik and M. Kloc, *Catalysis letters*, 2000, **64**, 41-47.
30 H. Jiang, X. Sun, M. Huang, Y. Wang, D. Li and S. Dong, *Langmuir*, 2006, **22**, 3358-3361.
31 D. Ichinohe, N. Saitoh and H. Kise, *Macromolecular Chemistry and Physics*, 1998, **199**, 1241-1245.
32 D. Ichinohe, T. Muranaka, T. Sasaki, M. Kobayashi and H. Kise, *Journal of Polymer Science Part A: Polymer Chemistry*, 1998, **36**, 2593-2600.
33 M. Stavola, D. Krol, W. Weber, S. Sunshine, A. Jayaraman, G. Kourouklis, R. Cava and E. Rietman, *Physical Review B*, 1987, **36**, 850-853.
34 C. Wagner, W. Riggs, L. Devis, J. Moulder and G. Muilenberg, *Phys. Elect. Div., Eden Prairie, Minnesota, USA*, 1979.
35 S. Wang, Z. Tan, Y. Li, L. Sun and T. Zhang, *Thermochimica Acta*, 2006, **441**, 191-194.
36 C. Yang and C. Chen, *Synthetic Metals*, 2005, **153**, 133-136.
37 X. Guo, G. T. Fei, H. Su and L. De Zhang, *Journal of Materials Chemistry*, 2011, **21**, 8618-8625.